GSA Data Repository 2016010

Hydrological thresholds and basin control over paleoflood records in lakes

Daniel N. Schillereff et al.

SUPPLEMENTAL METHODS

Trapping of sediments at Brotherswater

A detailed description of our sediment trapping methodology deployed at Brotherswater is provided in Schillereff (2015). In brief, cylindrical PVC tubes with an aspect ratio of 6.8:1 (0.75 m in length x 0.11 m diameter) were fitted with screw-thread removable 500 mL basal vessels. The dimensions follow the recommendations of Bloesch and Burns (1980) and Blomqvist and Håkanson (1981), optimised to ensure representative capture of sediment flux. At two mooring locations, delta proximal and distal, fixed pairs of replicate traps (following Ohlendorf and Sturm, 2001) were installed at three water depths i) near the lake bed, ii) at the seasonal metalimnion (6-8 m depth) and iii) in the surface waters at 4 m. The uppermost sediment trap carried a water depth logger (HOBO U20-001-04; manufacturer estimated accuracy ±0.44°C) recording lake water level and temperature every 10 minutes. The accumulated sediment dry masses were calculated after centrifuging to remove supernatant water and freeze drying the residues. Sediments were weighed and converted to mass accumulation rates (MAR) using: $W_D / d / (\pi * r^2)$, where W_D = dry sample mass, d = number of days between sampling and r = radius of the trap tube.

Hydrometeolorogical data

Total daily precipitation data were collected by tipping bucket rain gauge at the UK Environment Agency site at Hartsop Hall (#600140, 54.500°N 2.930°W; Figure 1a). Maximum daily discharge data were acquired from three different UK Environment Agency gauging stations downstream of Brotherswater moving through the River Eden headwaters: Patterdale Side Farm (#761511; in operation from CE 1997-present) on Goldrill Beck, the Brotherswater outflow, Pooley Bridge on the River Eamont (#76015; CE 1976-present) and Eamont Bridge on the River Lowther (#76004; CE 1962-present). These stations are progressively further downstream from Brotherswater but offer the longest and most comprehensive river flow records for comparison with the sediment records. Although individual floods differ between sites in terms of absolute magnitude, there is a strong correspondence in the occurrence of peak flows between stations across periods of overlapping monitoring (Figure DR4**)**.

Core chronology

Aliquots weighing 10 g after freeze-drying, sub-sampled at intervals of 1.5-2.5 cm (BW11-2) and 1-2 cm (BW12-9), were measured for the natural radionuclides ^{210}Pb and ^{226}Ra and the artificial isotopes ^{137}Cs and ^{241}Am by direct gamma assay in the Liverpool University Environmental Radioactivity Laboratory, following the procedures described in Appleby et al. (1986) (Figure DR1). Unsupported ^{210}Pb concentrations decline exponentially in both cores, assigning the following ages to the basal sediments presented here (Figures 3B, 4): CE 1938 ± 6 at 29.25 cm depth in BW11-2 and CE 1957 ± 4 at 11.25 cm in BW12-9. The presence of well-defined, concurrent peaks in ^{137}Cs and ^{241}Am concentrations at 21-23 cm (BW11-2) and 9.5-11 (BW12-9) record the CE 1963 peak in atmospheric radioactive material from nuclear weapons testing, and these markers corroborate the ^{210}Pb chronology. The shallower ^{137}Cs peaks identified in both cores (11-13 cm and 4-5.5 cm, respectively) are attributed to the CE 1986 Chernobyl accident, also conforms well to both ^{210}Pb age-depth models.

Appleby, P.G., Nolan, P.J., Gifford, D.W., Godfrey, M.J., Oldfield, F., Anderson, N.J., and Batterbee, R.W., 1986, 210Pb dating by low background gamma counting: Hydrobiologia, v. 143, p. 21–27.

Bloesch, J., and Burns, N., 1980, A critical review of sedimentation trap technique: Schweizerische Zeitschrift für Hydrologie, v. 42, no. 1, p. 15–55.

Blomqvist, S., and Håkanson, L., 1981, A review on sediment traps in aquatic environments: Archiv für Hydrobiologie, v. 91, p. 101–132.

Ohlendorf, C., and Sturm, M., 2001, Precipitation and dissolution of calcite in a Swiss High Alpine Lake: Arctic, Antarctic, and Alpine Research, v. 33, no. 4, p. 410–417.

Schillereff, D.N., 2015, A review of in situ measurement techniques for investigating suspended sediment dynamics in lakes, *in* Clarke, L. and Nield, J. eds., Geomorphological Techniques (Online Edition), British Society for Geomorphology, London, UK, p. 7.1.

SUPPLEMENTAL FIGURES

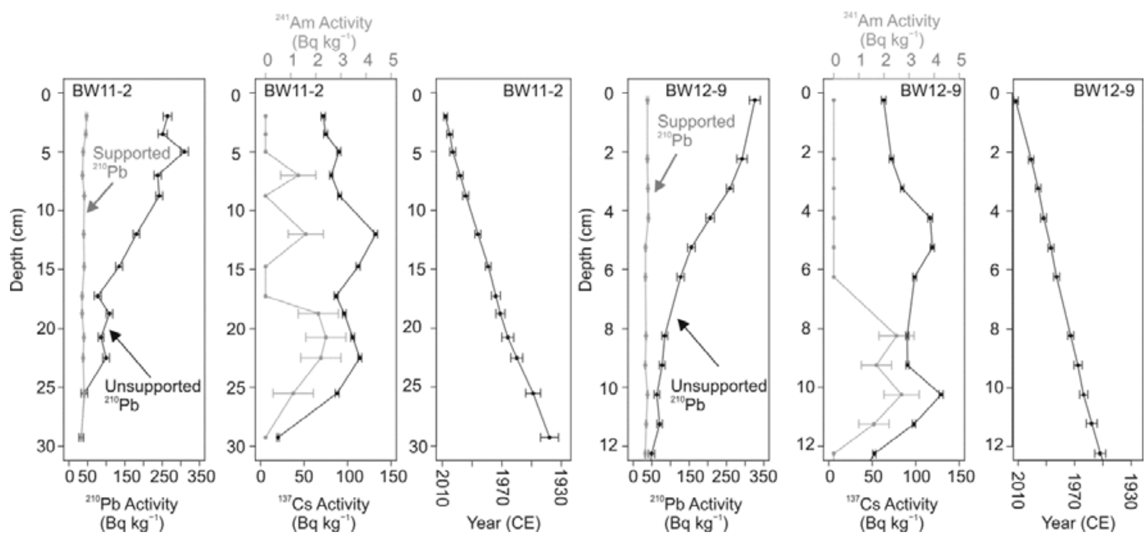

Figure DR1. Natural and artificial radionuclide measurements of ^{210}Pb, ^{137}Cs and ^{241}Am and the calculated sediment ages for cores BW11-2 and BW12-9.

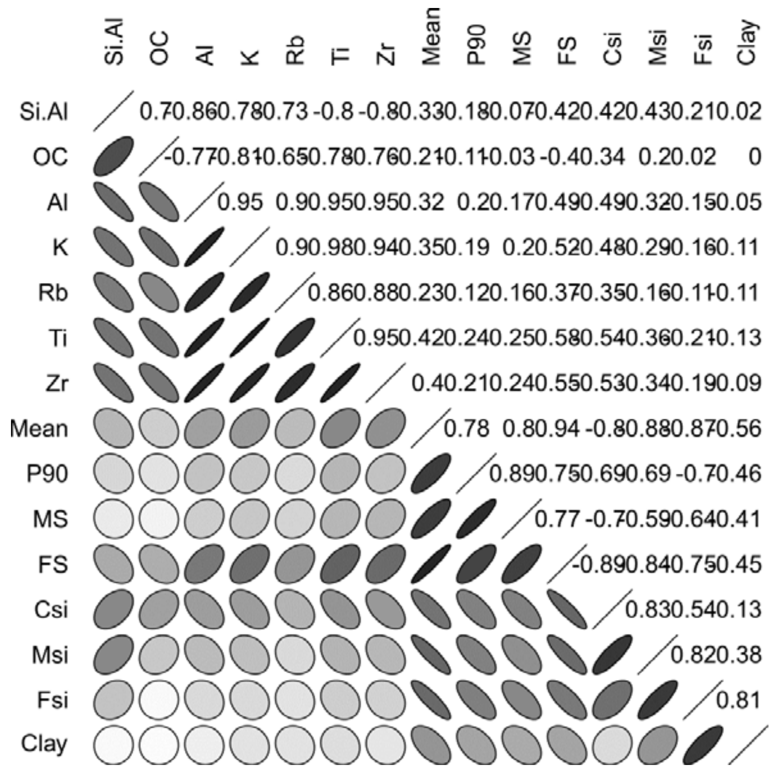

Figure DR2. Correlations between selected major and trace elements (concentrations), the Si/Al ratio (Si.Al), organic carbon content (OC), particle size fractions (mean = average grain size (μm), P90 = 90th percentile (μm), MS = medium sand, FS = fine sand, C/M/Fsi = coarse/medium/fine silt, and clay) displayed as shaded ellipses with the corresponding *R* value. The elements displayed are typically indicative of lithogenic sediment supply, but can reflect particle-size sorting within the lake (see text). The narrowness of each ellipse corresponds to the strength of the relationship (thin = higher *R*).

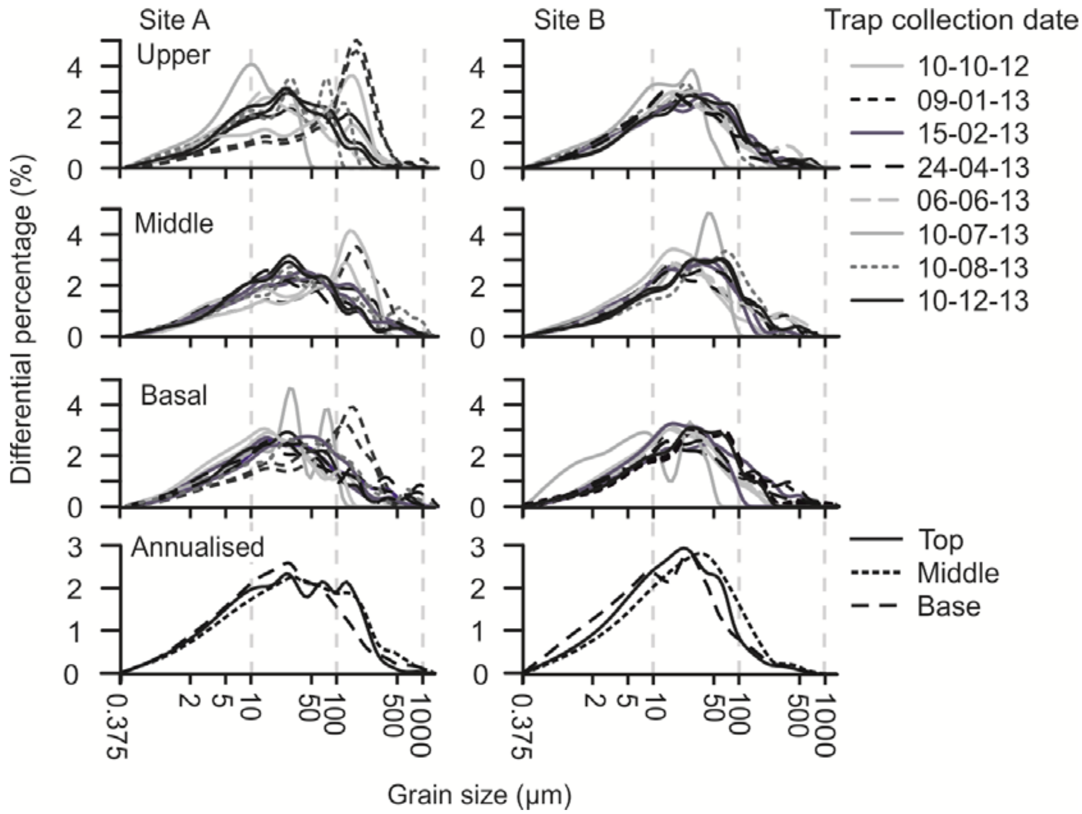

Figure DR3. Particle size distributions (PSD) of each sampling interval. The bottom plots present the time-normalised, cumulative PSD, representing material deposited through the full monitoring period.

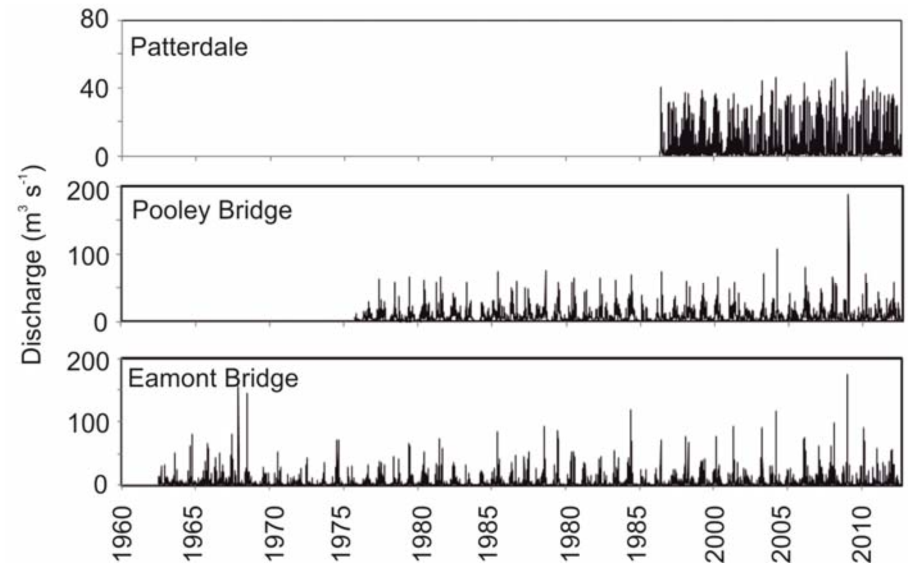

Figure DR4. Daily maximum discharges for the three gauging stations discussed in the text (locations presented in Figure 1). While the overall discharge increases down-catchment, the comparative scaling of peaks flows is consistent between stations during the overlap periods.

Table DR1. Dry weight and sediment mass accumulation rates (MAR) for each trap.

		Trap Depth					
		Top		**Middle**		**Base**	
Date deployed	**Date collected**	**Dry weight (g)**	**MAR (mg cm^{-2} d^{-1})**	**Dry weight (g)**	**MAR (mg cm^{-2} d^{-1})**	**Dry weight (g)**	**MAR (mg cm^{-2} d^{-1})**
<u>Site A</u>							
15 Aug 12	10 Oct 12	4.849	0.376	4.002	0.376	7.4866	0.703
10 Oct 12	9 Jan 13	6.030	0.349	4.850	0.280	5.222	0.302
9 Jan 13	15 Feb 13	N.D.	N.D.	2.969	0.422	4.473	0.636
15 Feb 13	24 Apr 13	N.D.	N.D.	1.040†	0.161†	8.466	0.655
24 Apr 13	6 Jun 13	0.855	0.102	N.D.	N.D.	5.846	0.699
6 Jun 13	10 July 13	0.269	0.042	0.371	0.056	2.914	0.487
10 July 13	10 Aug 13	3.158	0.536	4.112	0.698	5.205	0.883
10 Aug 13	10 Dec 13	3.421	0.148	3.832	0.165	2.662††	0.230†
<u>Site B</u>							
15 Aug 12	10 Oct 12	1.394	0.131	1.195†	0.225†	8.987	0.844
10 Oct 12	9 Jan 13	N.D.	N.D.	N.D.	N.D.	N.D.	N.D.
9 Jan 13	15 Feb 13	1.092	0.155	1.240	0.176	2.131	0.303
15 Feb 13	24 Apr 13	1.514	0.117	1.690	0.131	2.485	0.192
24 Apr 13	6 Jun 13	0.746	0.089	0.738	0.088	25.805	3.086
6 Jun 13	10 July 13	0.309	0.048	0.429	0.066	14.781	2.287
10 July 13	10 Aug 13	2.301	0.391	1.546	0.262	N.D.	N.D.
12 Aug 13	10 Dec 13	2.928	0.126	3.669	0.158	9.214	0.397

Note: *N.D. No recovery surface buoy submerged

† One of the pair was recovered